S1. Balance of flame surface density transport equation

In the present paper, the approach consists in defining a progress variable $\mathcal{C}$ as:

$$\mathcal{C} = \mathcal{H}(c - c^*), \tag{1}$$

where $\mathcal{H}(c)$ is the Heaviside function giving $\mathcal{C} = 0$ when $c < c^*$ and $\mathcal{C} = 1$ otherwise. Following the work of [1], the filtered transport equations of the CFM approach becomes:

$$\frac{\partial \overline{\rho}\widetilde{\mathcal{C}}}{\partial t} + \nabla \cdot (\overline{\rho}\widetilde{\mathbf{u}}\widetilde{\mathcal{C}}) = -\underbrace{\nabla \cdot \left(\overline{\rho \mathbf{u}\mathcal{C}} - \overline{\rho}\widetilde{\mathbf{u}}\widetilde{\mathcal{C}}\right)}_{T_1'} + \underbrace{\langle \rho S_d \rangle_{s,c^*} \overline{\Sigma^*}}_{T_2'}, \tag{2}$$

$$\begin{aligned}\frac{\partial \overline{\Sigma}^*}{\partial t} + \nabla \cdot (\widetilde{\mathbf{u}}\overline{\Sigma}^*) = &-\underbrace{\nabla \cdot \left(\overline{\mathbf{u}\Sigma^*} - \widetilde{\mathbf{u}}\overline{\Sigma}^*\right)}_{T_3'} + \underbrace{\langle \nabla \cdot \mathbf{u} - \mathbf{nn} : \nabla \mathbf{u} \rangle_{s,c^*} \overline{\Sigma}^*}_{T_4'} \\ &+ \underbrace{\langle S_d \kappa \rangle_{s,c^*} \overline{\Sigma}^*}_{T_5'} - \underbrace{\nabla \cdot \left(\langle S_d \mathbf{n} \rangle_{s,c^*} \overline{\Sigma}^*\right)}_{T_6'},\end{aligned} \tag{3}$$

where $\overline{\Sigma}^* = \overline{\Sigma \delta(c_c^*)}$ is the flame surface density (FSD) along the iso-surface of the progress variable at $c = c^*$. In these equations, 6 terms need to be closed:

1. The unresolved turbulent transport $T_1' = \nabla \cdot \left(\overline{\rho \mathbf{u}\mathcal{C}} - \overline{\rho}\widetilde{\mathbf{u}}\widetilde{\mathcal{C}}\right)$ in Eq. (2),
2. The surface averaged displacement speed weighted with density $\langle \rho S_d \rangle_{s,c^*}$ involved in T_2' (Eq. 2),
3. The unresolved turbulent transport $T_3' = \nabla \cdot \left(\overline{\mathbf{u}\Sigma^*} - \widetilde{\mathbf{u}}\overline{\Sigma}^*\right)$ in Eq. (3),

4. The tangential strain rate $\langle a_T \rangle_{s,c^*}$ involved in T_4' (Eq. 3),
5. The stretch due to curvature $\langle S_d \kappa \rangle_{s,c^*}$ involved in T_5' (Eq. 3),
6. The normal propagation term $T_6' = \nabla \cdot \left(\langle S_d \mathbf{n} \rangle_{s,c^*} \overline{\Sigma}^* \right)$ in Eq. (3).

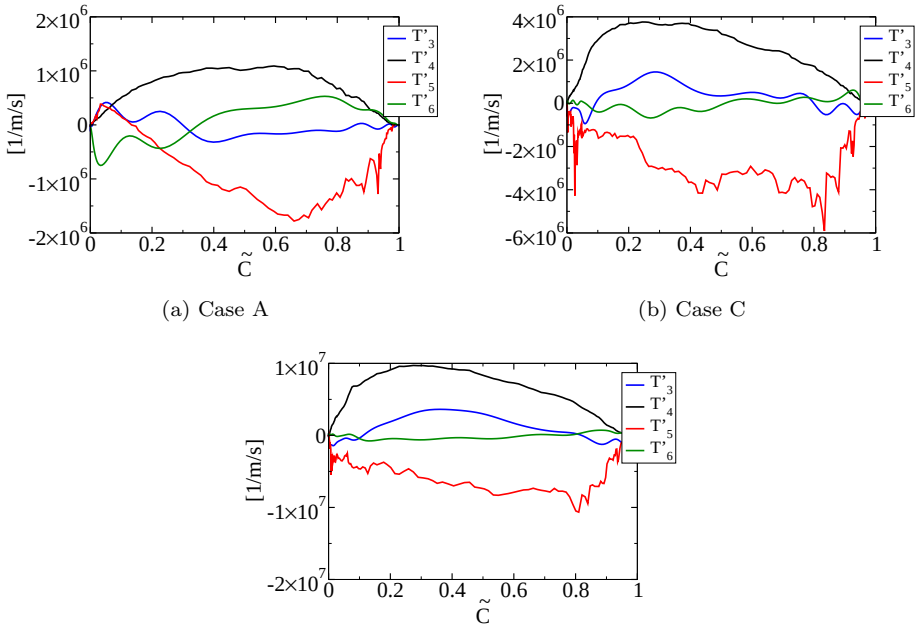

(a) Case A

(b) Case C

(c) Case D

Figure S.1: Comparison of the source terms involved in Eq. (3) as functions of $\widetilde{\mathcal{C}}$. T_3' is the unresolved transport term $\nabla \cdot \left(\overline{\mathbf{u}\Sigma^*} - \widetilde{\mathbf{u}}\overline{\Sigma}^* \right)$, T_4' is the source term related to tangential strain rate and T_5' is the source term related to stretch due to curvature $\langle S_d \kappa \rangle_{s,c^*}$ and T_6' is the normal propagation term $\nabla \cdot \left(\langle S_d \mathbf{n} \rangle_{s,c^*} \overline{\Sigma}^* \right)$.

Figure S.1 shows the unresolved transport term T_3', the flame surface density source terms T_4' and T_5', and the normal propagation T_6' as functions of $\widetilde{\mathcal{C}}$ for cases A, B and E, extracted from DNS using the procedure presented in Appendix C. In Fig. S.1, the terms T_3' and T_6' are approximately one order of magnitude smaller than T_4' and T_5' for each case.

S2. Supplementary materials for tangential strain rate modeling

S2.1. Derivation of the implified formula for $\langle a_T \rangle_{s,c^*}$

In the present paper, the model investigated for the tangential strain rate $\langle a_T \rangle_{s,c^*}$ is the following:

$$\langle a_T \rangle_{s,c^*} = \alpha_{a_T} \Gamma \frac{u'}{l_t}, \tag{4}$$

where α_{a_T} is a modeling constant. Function Γ is defined from the relationship existing between strain rate and energy spectrum in homogeneous turbulence:

$$\left(\Gamma \frac{u'}{l_t}\right)^2 = \left(\frac{\pi}{l_t}\right)^3 \int_1^\infty [C(k_+)]^2 k_+^2 E_{11}(k_+) dk_+, \tag{5}$$

where $k_+ = k l_t / \pi$ is the dimensionless wavenumber and $C(k_+)$ is an efficiency function, which takes into account the ability of the turbulent eddies at scale k to stretch the flame. $E_{11}(k_+)$ is the one-dimensional (longitudinal) energy spectrum in the direction of the wavenumber k, defined using the standard longitudinal Kolmogorov spectrum with the Pao correction to account for the viscous cut-off:

$$E_{11}(k_+) = \frac{18}{55} \left(\pi \frac{k_+}{l_t}\right)^{-5/3} \varepsilon^{2/3} \exp\left(-\frac{3}{2} C_k \left(\pi k_+ \frac{\eta}{l_t}\right)^{4/3}\right), \tag{6}$$

where $C_k \approx 1.5$ is the universal Kolmogorov constant, η is the Kolmogorov scale and ε is the rate of dissipation of TKE.

When a unit constant is used for the efficiency function $C(k_+)$ in Eq. (5),

the integration of Eq. (5) combined with Eq. (6) leads to :

$$\Gamma^2 = \left(\frac{9}{55}\right)\left(\frac{Re_t}{C_k}\right)\exp\left(-\frac{3}{2}C_k\frac{\pi^{4/3}}{Re_t}\right) \tag{7}$$

Then this expressionof Γ is introduced in Eq. (4) leading to:

$$\langle a_T\rangle_{s,c^*} = \alpha_{a_T}\left(\frac{3}{\sqrt{55}}\right)\sqrt{\frac{Re_t}{C_k}}\sqrt{\exp\left(-\frac{3}{2}C_k\frac{\pi^{4/3}}{Re_t}\right)}\left(\frac{u'}{l_t}\right). \tag{8}$$

Yet, $(u'/l_t)\sqrt{Re_t} = (u'/l_t)DaKa = (S_L^0/\delta_L^0)Ka$. In addition, by assuming that Re_t is sufficiently large, $\exp\left(-(3/2)C_k\pi^{4/3}/Re_t\right)$ is close to 1. Thus, by combining α_{a_T} and $1/\sqrt{C_k}$, the model for the tangential strain rate is:

$$\langle a_T\rangle_{s,c^*} = \alpha_{a_T}\frac{3}{\sqrt{55}}Ka\frac{S_L^0}{\delta_L}. \tag{9}$$

Similarly, introducing a Heaviside function with a cut-off scale δ_c as an efficiency function $C(k_+)$ in Eq. (5) leads to:

$$\begin{aligned}\Gamma^2 = \left(\frac{9}{55}\right)\left(\frac{Re_t}{C_k}\right)\Bigg[&\exp\left(-\frac{3}{2}C_k\frac{\pi^{4/3}}{Re_t}\right)\\ &-\exp\left(-\frac{3}{2}C_k\frac{\pi^{4/3}}{Re_t}\left(\frac{l_t}{\delta_L^0}\right)^{4/3}\right)\Bigg].\end{aligned} \tag{10}$$

With the same assumption on Re_t and similarly to Eq. (9), this expression of Γ leads to:

$$\langle a_T\rangle_{s,c^*} = \alpha_{a_T}\frac{3}{\sqrt{55}}Ka\frac{S_L^0}{\delta_L}\left[1-\exp\left(-\frac{3}{2}C_k\frac{1}{Re_t}\left(\frac{\pi l_t}{\delta_c}\right)^{4/3}\right)\right]^{1/2}. \tag{11}$$

S2.2. Sensitivity of LPF model to the cut-off scale

Equation (11) presents two modelling parameters, which gives more latitude to fit the model to DNS results. Figure S.2 shows the sensitivity to δ_c of Eq. (11) by choosing δ_c between $(1/2)\delta_L^0$ and $2\delta_L^0$. This range for the cut-off length correspond to realistic values. As for the results presented in the present paper, the values of the model parameter α_{a_T} used are adjusted to fit the lowest Karlovitz nulmber cases using the model proposed by Charlette *et al.* [2]. This figure shows that choosing δ_c between $(1/2)\delta_L^0$ and $2\delta_L^0$ still

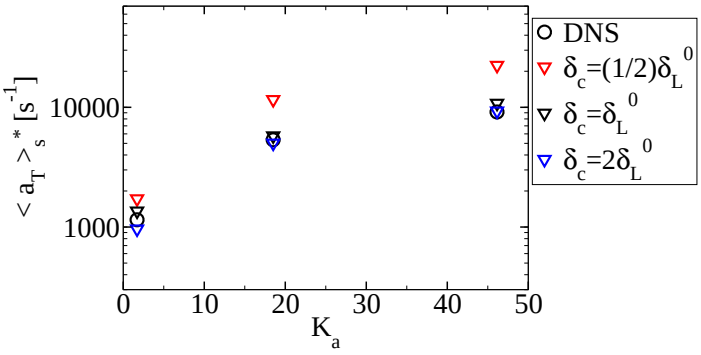

(a) $Le = 1$

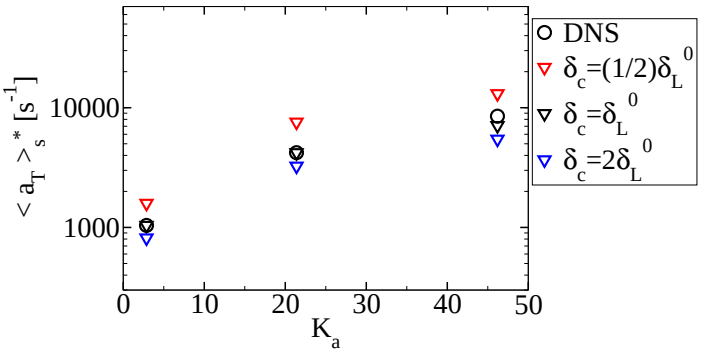

(b) $Le > 1$

Figure S.2: Tangential strain rate $\langle a_T \rangle_s^*$ from DNS compared to LPF model using $(1/2)\delta_L^0$, δ_L^0 and $2\delta_L^0$: (a) for cases with $Le = 1$ and (b) for cases with $Le > 1$.

gives the best results without adjusting constant α_{a_T}. In addition, this shows

that the model sensitivity to δ_c is low.

S2.3. α_{a_T} tuning

In the present paper, the different models investigated for tangential strain rate $\langle a_T \rangle_{s,c^*}$ are compared by tuning the model parameter α_{a_T} on cases A and A_1 using Charlette's model [2].

A comparison of $\langle a_T \rangle_s^*$ extracted from the DNS with the models is then presented in Fig. S.3 for all DNS cases but by tuning for each model the parameter α_{a_T} to fit the strain rate obtained at the lowest Karlovitz numbers (i.e., cases A and A_1). This tuned parameter is reported in Table S.1 for each model.

Table S.1: Tuned model parameter α_{a_T} for each model.

	Bougrine	Cant	Charlette	HK_{2D}	LPF
$Le_k \neq 1$	10.6	0.8	1.7	1.2	1.4
$Le_k = 1$	7.1	1.6	2.8	1.1	2.4

Figure S.3 shows that tuning α_{a_T} for each model improves significantly the predictions. The conclusions drawn in the analysis presented in the current paper are still valid when α_{a_T} is tuned for each model. Figure S.3 shows that the best model is the LPF model and choosing δ_L^0 as the cut-off scale seems appropriate.

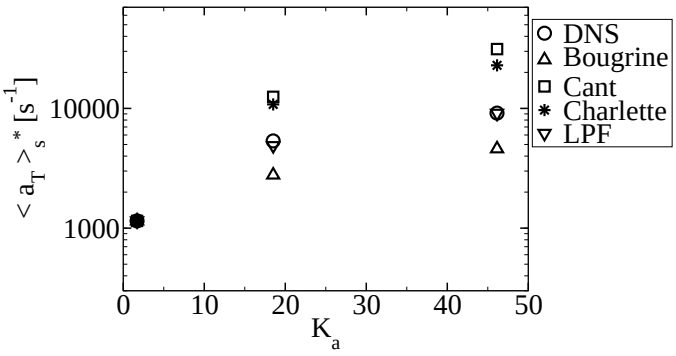

(a) $Le = 1$

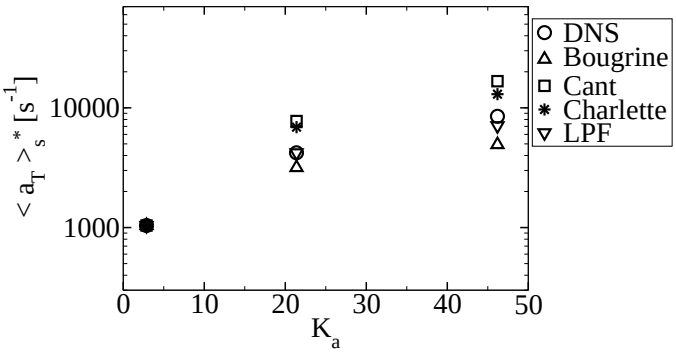

(b) $Le > 1$

Figure S.3: Tangential strain rate $\langle a_T \rangle_s^*$ from DNS compared to Bougrine's model [3], Cant's model [4], Charlette's model [2] and LPF model: (a) for cases with $Le = 1$ and (b) for cases with $Le > 1$. Each model is tuned to fit the lowest Karlovitz number case.

References

[1] E. Knudsen, H. Pitsch, A dynamic model for the turbulent burning velocity for large eddy simulation of premixed combustion, Combustion and Flame 154 (4) (2008) 740–760. doi:10.1016/j.combustflame.2008.05.024.

URL https://doi.org/10.1016/j.combustflame.2008.05.024

[2] F. Charlette, C. Meneveau, D. Veynante, A power-law flame wrinkling model for les of premixed turbulent combustion part i: Non-dynamic formulation and initial tests, Combustion and Flame 131 (1-2) (2002) 159–180. doi:10.1016/S0010-2180(02)00400-5.

[3] S. Bougrine, S. Richard, O. Colin, D. Veynante, Fuel composition effects on flame stretch in turbulent premixed combustion: Numerical analysis of flame-vortex interaction and formulation of a new efficiency function, Flow, turbulence and combustion 93 (2) (2014) 259–281.

[4] R. Cant, S. Pope, K. Bray, Modelling of flamelet surface-to-volume ratio in turbulent premixed combustion, Symposium (International) on Combustion 23 (1) (1991) 809–815.